

Article

High-Power Ultrasonic Synthesis and Magnetic-Field-Assisted Arrangement of Nanosized Crystallites of Cobalt-Containing Layered Double Hydroxides

Andrei N. Salak ^{1,*}, Daniel E. L. Vieira ¹, Irina M. Lukienko ², Yuriy O. Shapovalov ², Alexey V. Fedorchenko ², Elena L. Fertman ², Yuriy G. Pashkevich ^{2,3}, Roman Yu. Babkin ³, Aleksandr D. Shilin ⁴, Vasili V. Rubanik ⁴, Mário G. S. Ferreira ¹ and Joaquim M. Vieira ¹

¹ Department of Materials and Ceramics Engineering, CICECO—Aveiro Institute of Materials, University of Aveiro, 3810-193 Aveiro, Portugal

² B. Verkin Institute for Low Temperature Physics and Engineering of the National Academy of Sciences of Ukraine, 47 Nauky Ave., 61103 Kharkov, Ukraine

³ O. Galkin Donetsk Institute for Physics and Engineering of the National Academy of Sciences of Ukraine, 46 Nauky Ave., 03680 Kyiv, Ukraine

⁴ Institute of Technical Acoustics of National Academy of Sciences of Belarus, Lyudnikov Avenue, 13, 210009 Vitebsk, Belarus

* Correspondence: salak@ua.pt; Tel.: +351-234-247318

Received: 11 May 2019; Accepted: 3 July 2019; Published: 4 July 2019



Abstract: High-quality stoichiometric $\text{Co}_2\text{Al-NO}_3$ and $\text{Co}_2\text{Al-CO}_3$ layered double hydroxides (LDHs) have been obtained by precipitation followed by anion exchange, both high-power-sonication assisted. Application of high-power ultrasound has been demonstrated to result in a considerable acceleration of the crystallization process and the anion-exchange reaction. Two independent approaches were used to form bulk and 2-D samples of $\text{Co}_2\text{Al-NO}_3$ with the oriented crystallites, namely uniaxial pressing of deposits from sonicated LDH slurries and magnetic field-assisted arrangement of LDH crystallites precipitating on glass substrates. A convenient way of preparation of semi-transparent compacts with relatively big blocks of oriented crystallites have been demonstrated. Thin dense transparent films of highly-ordered crystallites of $\text{Co}_2\text{Al-NO}_3$ LDH have been produced and characterized.

Keywords: magnetic layered structure; oxygen octahedron; anisotropic crystallite; highly-ordered arrangement

1. Introduction

Layered double hydroxides (LDHs) of the $\text{M}^{2+}\text{-M}^{3+}$ type represent the most numerous group in the anion clays family [1]. Although some of them occur as natural minerals, most of the known LDHs are synthetic. Their framework is composed of parallel positively-charged layers of the double metal hydroxides, $[\text{M}^{2+}_{1-x}\text{M}^{3+}_x(\text{OH})_2]^{x+}$, where $0.17 \leq x \leq 0.50$ [2]. The positive charge of the hydroxide layer is compensated by anions (A^{y-}) intercalated into the interlayer gallery and screened from each other by water molecules [2]. To denote the chemical composition of an LDH, a short form, namely $\text{M}^{2+}_n\text{M}^{3+}\text{-A}^{y-}$, where $n = (1 - x)/x$ is the atomic ratio of the cations M^{2+} and M^{3+} in the layer, is commonly used. Owing to the complex electrostatic interaction between hydroxide layers and the interlayer species, LDHs can be intercalated with anions and anionic complexes, which are very different in nature, size, geometry and charge [2–9]. Moreover, the same anions in the interlayer of the same LDH can be arranged in several ways depending on the cations ratio [9] and on the relative

amount of intercalated water [10] that results in different distances between the adjacent hydroxide layers (basal spacings).

Layered double hydroxides are widely used in catalysis; however, the general applications of LDHs are resulted from their unique anion-exchange ability [3]. In their capacity of exchangers and adsorbents, LDHs are extensively used as (nano)containers for delivery of drugs, genes and markers in vivo [11–14], active pigments in coatings for corrosion protection [15–17], agents in the systems for water purification [18–20] and in other areas. In such applications, the nature of cations M^{2+} and M^{3+} is disregarded (except for apparent aspects of low cost and ecological compatibility), since in respect of anion-exchange properties the M^{2+}/M^{3+} ratio is only important since it entirely determines the layer charge per unit cell [21].

Functionalities of LDHs can be extended by means of a use of particular cations in the hydroxide layers. Luminescence properties of LDHs with M^{3+} partly substituted by rare earth cation [22–24] have recently been reported. The layered double hydroxides, in which at least one of the metal cations is magnetic: Co^{2+} , Ni^{2+} , Mn^{3+} , Cr^{3+} or Fe^{3+} , were studied [25–33]. Onset of spontaneous magnetization and a peak of magnetic susceptibility were observed in those LDHs at temperatures of a few K. The highest T_C of 26 K was reported for Ni_4Mn-CO_3 LDH [28]. Because of the very low T_C values, direct practical exploration of the magnetic transition in such materials is unlikely. Nevertheless, some features of such magnetic LDHs, in particular the tunability of their magnetism via the layer cation content, the cation ratio and the interlayer distance can be used in preparation of functional materials. Coronado and co-workers have published several successful examples of the application of layered double hydroxides in formation of magnetic hybrids [29–32].

Unusual magnetic behavior of LDHs containing Co^{2+} , namely Co_2Al-NO_3 and Co_3Al-NO_3 in the temperature range above liquid nitrogen has recently been reported. Specifically, between about 80 and 150 K, both the paramagnetic Curie temperature and the effective magnetic moment were found to vary in a non-monotonous way [34]. Based on a detailed consideration of crystal structure and modeling, Babkin et al. have shown that freezing of tilting fluctuations of O–H bonds are responsible for these anomalies [35]. Taking into account the statistical distribution of divalent and trivalent cations, and their effect on the distortions of the original structure, the temperature dependences of the magnetic susceptibility of Co_nAl-NO_3 LDHs ($n = 2,3,4$) were calculated. It was noted that cobalt-containing LDHs represent convenient models for experimental modeling of effects of frustrated magnetic states in solids.

Unfortunately, the maximum size of the LDH crystallites, which are flake-like with the typical diameter-to-thickness ratio of about 20:1, usually does not exceed 1–2 μm ; in the case of Co_nAl layered hydroxides, it is generally 50–100 nm [34]. Nevertheless, Abellán et al. [32] and Carrasco et al. [33] have prepared Co_2Al LDHs with relatively big (micrometric-size) regularly shaped crystallites.

The main problem that makes difficult any manipulations with individual LDH crystallites is their strong tendency to form shapeless agglomerates. The research group of Evans and Duan reported a use of a 0.2 μm membrane to filter the Co_3Fe LDH suspension with crystallites of about 100 nm in diameter, which then were assembled in an external magnetic field [36]. As a result, LDH–porphyrin composite film has been formed with a promising potential in application as an electrochemical sensor for glucose [37].

Co^{2+} -containing LDHs are generally produced using either the conventional co-precipitation methods (with the total duration of about 48 h) [31,32,34] or the hydrothermal synthesis (at least 24 h at 100–130 °C long) [33] or a combination of both [36,37]. Layered hydroxides synthesized in such ways contain anions of the initial metal salts or with other anions, which are present or created in the reaction solution. In the majority of applications, LDHs must be intercalated with functional anions: bioactive substances, corrosion inhibitors etc. The intercalation is implemented by means of anion exchange in the respective solutions. Complete substitution of the parent anions by functional ones takes from few hours to several days and even weeks depending on the anion's nature.

In this work, high-power sonication was applied at different stages of the Co_2Al-NO_3 synthesis and the nitrate-to-carbonate anion exchange processes in order to accelerate the LDH production.

For comparison, the same LDH compositions were obtained using the conventional co-precipitation procedure followed by anion exchange. Besides, we used the sonication treatment to de-agglomerate the obtained LDH crystallites and to facilitate their arrangement on a substrate.

The main objective of this work was to order and assemble crystallites of $\text{Co}_2\text{Al-NO}_3$ and $\text{Co}_2\text{Al-CO}_3$ LDHs with an assistance of an external magnetic field. The composition with the $n = 2$ cations ratio was chosen because the parent Co_2Al layered double hydroxides with this n value (i) are the easiest to obtain reproducibly and (ii) allow simple exchanges for numerous inorganic and organic anions. We have obtained semi-transparent compacts and transparent thin films of the arranged LDH crystallites and characterized them with respect to their morphology and some optical properties.

2. Materials and Methods

Cobalt (II) nitrate hexahydrate ($\geq 98\%$), aluminum nitrate nonahydrate ($\geq 98.5\%$), sodium hydroxide ($\geq 98\%$), sodium nitrate ($\geq 99.5\%$), sodium carbonate ($> 99.95\%$) were purchased from Sigma-Aldrich, while nitric acid (65%) was purchased from Merck. The chemicals were used as received without further purification. All the solutions were prepared in deaerated water. The co-precipitation procedure was carried out under a nitrogen atmosphere. Proportions of the reagents were chosen to meet the desired molar cation ratio ($\text{Co/Al} = 2$) without any excess.

To prepare $\text{Co}_2\text{Al-nitrate}$ LDH using the conventional method, a solution containing 0.5 M $\text{Co}(\text{NO}_3)_2 \cdot 6\text{H}_2\text{O}$ and 0.25 M $\text{Al}(\text{NO}_3)_3 \cdot 9\text{H}_2\text{O}$ was instilled to a 1.5 M NaNO_3 solution under continuous stirring at room temperature. During the precipitation, pH of the mixture was controlled by addition of a 2 M NaOH solution to be 8. This process took about one hour.

The obtained suspension was kept in a water bath at about 100°C for 4 h to complete the crystallization and then centrifuged at 10^4 rpm for 90 s. The resulting dense slurry was washed with deionized water followed by centrifugation. This procedure was repeated three times to remove a residual NaNO_3 .

Sonication-assisted experiments were performed using a VCX 1500 Sonics processor (max output power 1.5 kW at 20 kHz) equipped with a modified high-volume continuous flow cell.

High-power sonication was applied at three different stages of the LDH production, namely (1) at co-precipitation (synthesis) step, (2) at crystallization step and (3) at anion-exchange stage. A certain amount of the suspension/slurry obtained after each step was centrifuged, washed and dried as described above then used for the phase analysis.

In the first experiment, it was attempted to substitute the relatively long co-precipitation step by the sonication-assisted direct synthesis. The solutions of $\text{Co}(\text{NO}_3)_2 \cdot 6\text{H}_2\text{O}$, $\text{Al}(\text{NO}_3)_3 \cdot 9\text{H}_2\text{O}$, NaNO_3 and NaOH in the same amounts as those used for the conventional co-precipitation were mixed under a 1.5 kW ultrasonic agitation for 3, 5 or 10 min.

In the second experiment, the $\text{Co}_2\text{Al-NO}_3$ LDH slurry was sonicated at 1.5 kW for 2, 5 and 10 min just after the conventional co-precipitation step (without crystallization in a water bath).

The third experiment was conducted aiming at acceleration of the nitrate-to-carbonate anion-exchange reaction. The $\text{Co}_2\text{Al-NO}_3$ LDH slurry after the co-precipitation and the crystallization in a water bath was mixed with a 0.1 M NaCO_3 solution at room temperature. The pH value of the mixture was adjusted to be 8 using a 2 M NaOH solution. The obtained solution was sonicated at 1.5 kW for 7 min and then centrifuged at 10^4 rpm for 90 s. The LDH slurries prepared using the aforementioned procedures were estimated to contain about 85% of water.

For the phase analysis and the crystal structure characterization, the final product was dried at 60°C for 24 h. The X-ray diffraction (XRD) data of the obtained LDH powders were collected using a Rigaku D/MAX-B diffractometer equipped with a graphite monochromator to reduce contributions caused by fluorescence of cobalt in $\text{Cu K}\alpha$ radiation.

Two types of the samples, namely bulk samples (pressed compacts of LDH powders) and thin films (layers of the arranged LDH crystallites) were prepared with assistance of an external magnetic field. The experimental procedure was the following. A slurry of $\text{Co}_2\text{Al-NO}_3$ or $\text{Co}_2\text{Al-CO}_3$ LDH

produced using the conventional co-precipitation route followed by 4-min high-power sonication was dispersed in ethanol. The procedure was carried out in ultrasonic bath for 15 min. For the bulk samples preparation, the slurry-to-ethanol ratio was 0.05 g/mL, while the thin films were deposited using the suspension with the ratio of 0.01 g/mL. Immediately after the ultrasonic treatment, the suspension was put in a flat 10 mm height plastic container with a $15 \times 15 \times 0.5$ mm glass substrate at the bottom. The container was placed horizontally between the vertically oriented poles of a GMW Model 3470 electromagnet connected to an Agilent Model 6811B Power Source/Analyzer. The magnetic field generated in the pole gap was 0.5 T. The field was applied in three cycles of 1 min each. The cycles were divided into pulses of 10 s for the first minute and 20 s for the next two cycles. Then the substrate with the precipitated LDH was dried in the oven at 60 °C until the complete evaporation of ethanol. For comparison, the samples were also prepared using the same conditions in a zero magnetic field.

To prepare the bulk samples, thick layers of the deposited LDH particles were carefully removed from the glass substrate, placed on the die of a 6 mm cylindrical mold and pressed into semi-transparent slabs of about 0.30 mm thick. Some as-pressed samples were additionally polished to achieve better transparency.

Morphology of the deposited LDH layers was studied using a Hitachi S4100 scanning electron microscope (SEM) with an electron beam accelerating voltage of 25 kV. Size and morphology of the LDH particles/crystallites were characterized using a Hitachi HD-2700 scanning transmission electron microscope (STEM) with an electron beam accelerating voltage of 200 kV.

3. Results and Discussion

XRD patterns of the $\text{Co}_2\text{Al-NO}_3$ LDH samples synthesized from a mixture of the respective nitrates either using the conventional co-precipitation route or by means of ultrasonic agitation of the mixture are shown in Figure 1.

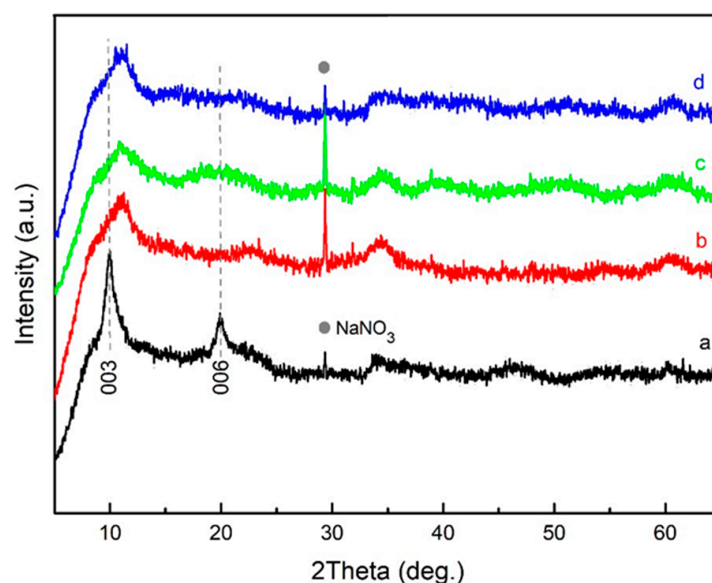


Figure 1. X-ray diffraction (XRD) patterns of the $\text{Co}_2\text{Al-NO}_3$ layered double hydroxides (LDHs) synthesized using the conventional co-precipitation method (a) and by means of the ultrasonic treatment of the stoichiometric mixture of the respective metal nitrates at 1.5 kW for 3 min (b), 5 min (c), and 10 min (d) followed by 4-h thermal treatment in a water bath. The strongest peak of the residual sodium nitrate (from the parent solution) is indicated.

It is seen from Figure 1 that in all the cases when sonication-assisted direct synthesis from the mixture of the respective nitrates was attempted the $\text{Co}_2\text{Al-NO}_3$ LDH phase was not formed regardless of the sonication treatment time. Although the most intense diffraction reflections associated with

LDH structure were seen in the XRD patterns (Figure 1b–d), these reflections broadened and were shifted with respect to those typical of $\text{Co}_2\text{Al-NO}_3$ (Figure 1a). When one prepares LDH using the conventional co-precipitation route, the synthesis goes rather slowly, taking about 1–2 hours and requires constant control and correction of pH. In the case of the direct sonication-assisted synthesis attempted in this work, in spite of the fact that the pH value was adjusted to the desired one in the starting mixture, it was impossible to control pH in the course of the high-power ultrasound treatment. We suggest that the pH value unpredictably changed during the sonication and this could have led to deviation in the cations ratio in the resulting LDH material as well as to intercalation of hydroxide anions together with (or instead of) nitrate anions.

A water bath thermal treatment of the suspension obtained by the co-precipitation is an important stage of formation of an LDH. At this stage, the LDH crystallite size is equalized. We have attempted to substitute this 4-hour stage by a high-power sonication for several minutes. XRD patterns of the respective LDHs are shown in Figure 2.

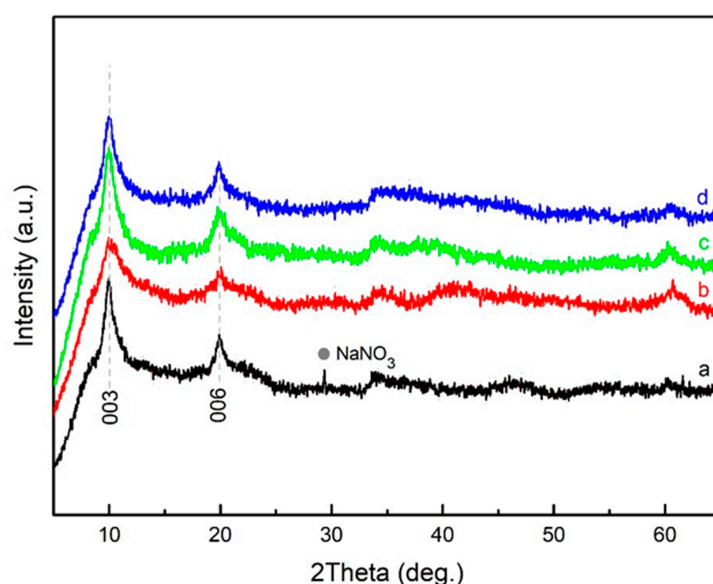


Figure 2. XRD patterns of the $\text{Co}_2\text{Al-NO}_3$ LDHs synthesized using the conventional co-precipitation method and then either kept in a water bath at about $100\text{ }^\circ\text{C}$ for 4 h (a) or sonicated at 1.5 kW for 2 min (b), 5 min (c), and 10 min (d).

One can see in Figure 2 that the XRD patterns of the samples obtained after the high-power sonication treatment of the LDH suspension are similar to the XRD pattern of the $\text{Co}_2\text{Al-NO}_3$ LDH prepared from the same suspension using a water bath treatment. The similarity of the patterns is especially evident for the sample sonicated for 5 min. Hence, a 4-h stage of the water bath treatment can be effectively substituted by a 5-min sonication stage. We suggest that a considerable reduction of the LDH crystallization is possible due to the acoustic cavitation caused by high-power sonication [38]. Acoustic cavitation is the formation, growth and collapse of bubbles in a liquid under the influence of an ultrasonic field [39]. The implosive collapse of the bubbles produces a localized heating area via shock wave formation (adiabatic compression) within the gas phase of the collapsing bubble.

The results obtained in our experiment on the sonication-assisted crystallization of LDHs are in agreement with those reported in previous works on the preparation of nanomaterials using the ultrasonic waves [40–42]: indeed, application of high-power ultrasound considerably accelerates chemical processes in aqueous solutions.

Figure 3 shows the XRD patterns of the $\text{Co}_2\text{Al-NO}_3$ LDH before and after the nitrate-to-carbonate exchange in the solution of Na_2CO_3 and NaOH under high-power sonication for 7 min. The XRD pattern of the material obtained as a result of such a treatment corresponded entirely of that of

Co₂Al–CO₃. It should be stressed here that the standard NO₃[−] → CO₃^{2−} anion-exchange reaction in Co₂Al–NO₃ takes about seven days of continuous stirring at room temperature.

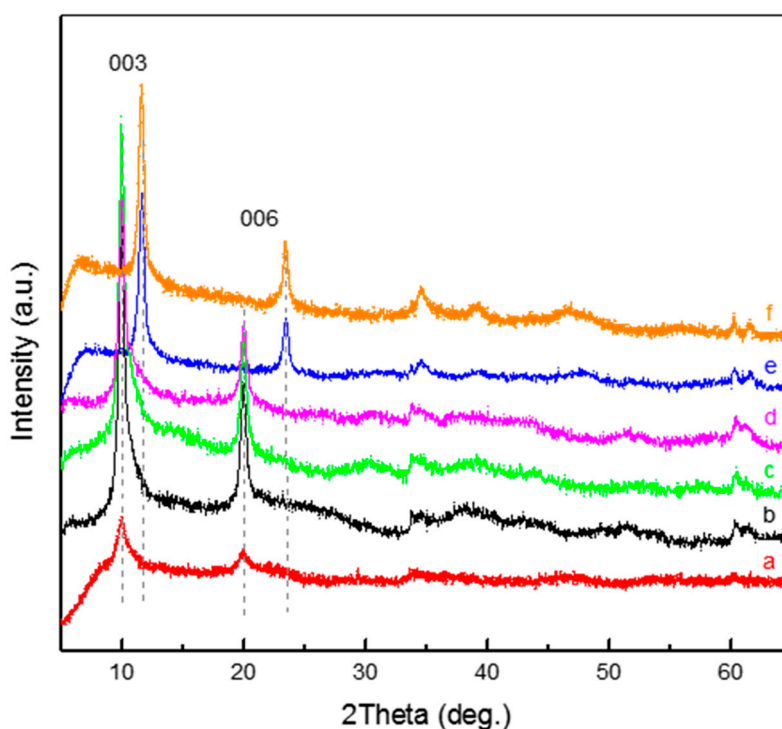


Figure 3. XRD patterns of the Co₂Al–NO₃ LDH prepared using the conventional co-precipitation method before (a), after the NO₃[−] → CO₃^{2−} anion-exchange reaction at room temperature either without sonication for 7 min (b), 60 min (c), 24 h (d) and 7 days (f) or under a 1.5 kW sonication for 7 min (e).

Such a considerable reduction of the time required to complete the anion-exchange reaction makes an application of the high-power sonication very promising.

It is known that anion-exchange is rather a diffusion process. We suggest that the high-power ultrasonic treatment enhances significantly the “interlayer diffusion” owing to both the local heating and the mechanical impacts on the hydroxide layers.

Lattice parameters (in a hexagonal setting) and basal spacings calculated from the 2Theta positions of the diffraction reflections (003), (006) and (110) for all the LDH compositions prepared in this work are listed in Table 1.

Table 1. Lattice parameters (*a*, *c*) and basal spacings (*d*) of the Co₂Al LDHs prepared via the conventional co-precipitation synthesis followed by anion-exchange and by means of the sonication-assisted procedures.

LDH Composition		<i>a</i> (Å)	<i>c</i> (Å)	<i>d</i> (Å)
Co ₂ Al–NO ₃	Conventional co-precipitation followed by 4-h crystallization in a water bath	3.063	26.732	8.911
Co ₂ Al–NO ₃ (sonication-assisted crystallization)	2 min	3.049	26.585	8.862
	5 min	3.071	26.579	8.860
	10 min	3.054	26.513	8.838
Co ₂ Al–CO ₃	Standard anion-exchange (7 days)	3.072	22.878	7.626
	Sonication-assisted exchange (7 min)	3.070	22.831	7.610

The relative errors in determination of the parameters *a* and *c* were 0.07% and 0.1%, respectively.

One can see that the values of lattice parameters of the same LDH compositions prepared using either the conventional routes or the sonication-assisted procedures were rather similar. However, in cases of the application of high-power sonication, the values of lattice parameters were regularly lower. This can be caused by some deviations from the desired cations ratio, $\text{Co}/\text{Al} = 2$. It should be noticed that the lattice parameters values for $\text{Co}_2\text{Al}-\text{CO}_3$ LDHs available from the literature are even lower than those obtained in our study (Table 1): cf.: $a = 3.066 \text{ \AA}$, $c = 22.593 \text{ \AA}$ [43] and $a = 3.068 \text{ \AA}$, $c = 22.609 \text{ \AA}$ [44].

An optical image (in nonpolarized light) of a pressed compact of $\text{Co}_2\text{Al}-\text{NO}_3$ layered double hydroxide powder precipitated in an external magnetic field and then dried without mixing is shown in Figure 4a. For comparison, the respective image of a compact of the same LDH composition prepared using the conventional route followed by centrifugation, drying and mixing with mortar and pestle is demonstrated in Figure 4b.

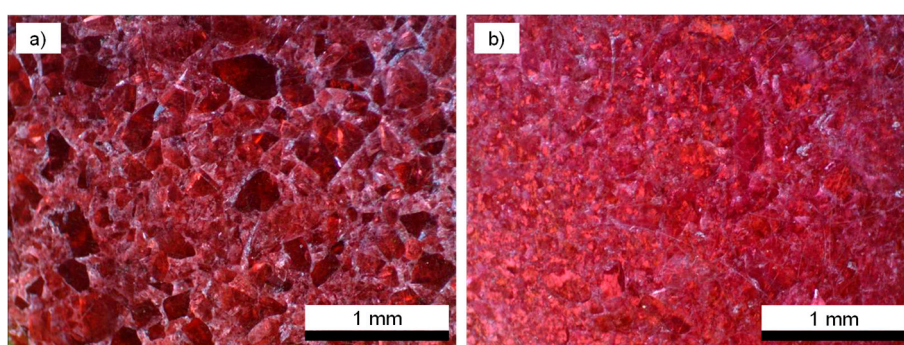


Figure 4. Images of the $\text{Co}_2\text{Al}-\text{NO}_3$ samples in nonpolarized light: the pressed compact of the LDH powder precipitated in an external magnetic field and then dried without mixing (a) and the pressed compact of the LDH powder dried after centrifugation (b).

Relatively big (up to 0.5 mm long) individual blocks with the same contrast are clearly seen in the samples pressed from the LDH powder deposited in an external magnetic field. Similar blocks are also observed in the $\text{Co}_2\text{Al}-\text{NO}_3$ sample pressed from the powder dried without precipitation in the field; however, their average size is considerably smaller. The same difference between average dimensions of the blocks visible in nonpolarized light was found in the respective compacts of $\text{Co}_2\text{Al}-\text{CO}_3$ LDHs.

Figure 5 shows the polarized light images of the $\text{Co}_2\text{Al}-\text{CO}_3$ compacts prepared from the LDH crystallites precipitated with and without an external magnetic field. The samples under study were polished to achieve thickness of about 0.15 mm.

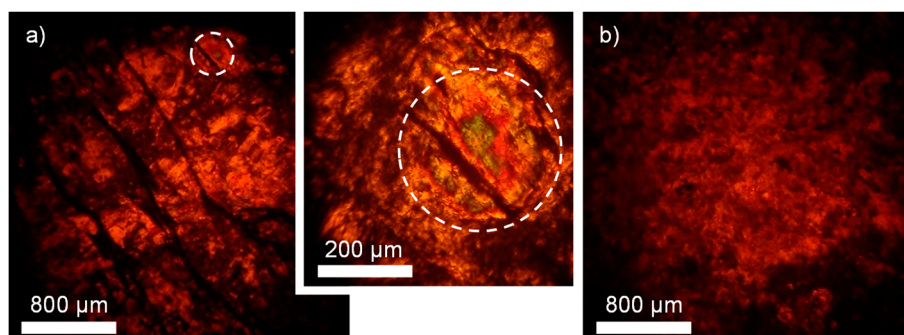


Figure 5. Images of the $\text{Co}_2\text{Al}-\text{CO}_3$ samples in a polarized microscope: the pressed compact of the LDH powder precipitated in an external magnetic field and then dried without mixing (a) and the pressed compact of the LDH powder dried after centrifugation (b). Inset shows the magnified image of the zone with the iridescent colors.

Since the thickness of these two samples is almost the same, their images in crossed polarizers can be compared by contrast. A higher contrast between dark and light areas suggests more homogeneous crystallite blocks (Figure 5). It is seen that the blocks of the sample prepared using the magnetic field assisted approach are bigger and more homogeneous than those in the sample produced via the conventional route. Iridescent color of some blocks is a manifestation of birefringence.

Figure 6 shows images of the zone with the iridescent colors observed in the $\text{Co}_2\text{Al}-\text{CO}_3$ sample (inset in Figure 5a) pressed from the powder precipitated in an external magnetic field and then dried without mixing. The observed variation in brightness of colored parts the crystallite block was caused by a tilted orientation of its optical axis.

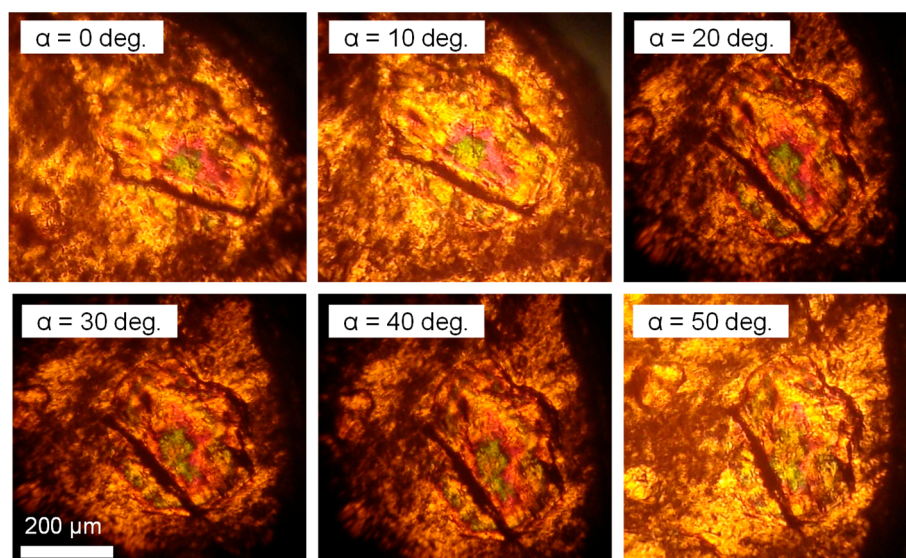


Figure 6. Images of the $\text{Co}_2\text{Al}-\text{CO}_3$ LDH compact (the same sample that shown in Figure 5a) in crossed polarizers. The turning angles of the sample in the microscope stage (α) are indicated.

These preliminary results suggest a good potential of this approach to produce relatively big self-supporting samples with oriented LDH crystallites.

Crystallites of the obtained $\text{Co}_2\text{Al}-\text{NO}_3$ were observed to be hexagon-shaped (Figure 7), which is typical for the rhombohedral LDHs.

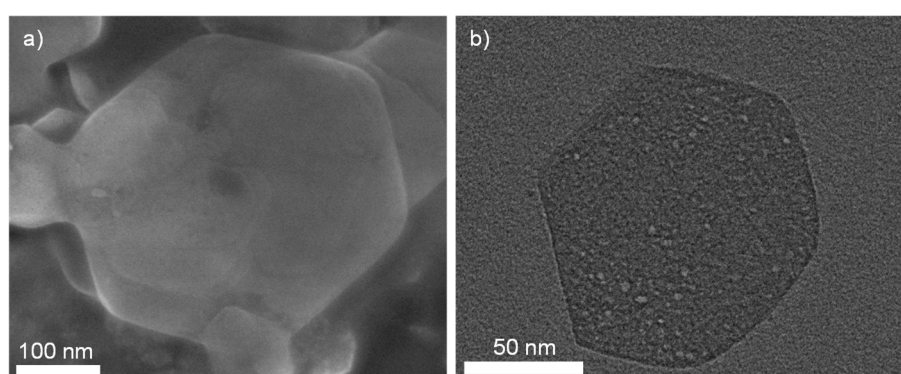


Figure 7. Electron microscope images of typical crystallites of $\text{Co}_2\text{Al}-\text{NO}_3$ LDH were taken in scanning mode (a) and in scanning transmission mode (b).

Free precipitation of LDH crystallites from water suspension is known to result in formation of big shapeless particles that consist of hundreds and even thousands of the crystallites [31]. If the LDH particles were dispersed in ethanol, agglomeration was mainly suppressed. Nevertheless, when an

external magnetic field was not applied, the LDH crystallites precipitated randomly (Figure 8b,d). The application of pulsed magnetic field promoted a formation of a dense homogenous layer of the flat-laying crystallites on a surface of the substrate (Figure 8a,c). One should notice that owing to a compact arrangement of the LDH crystallites the obtained film was thinner by about a factor of four than that in the case of randomly oriented crystallites.

It has been found that the crystallites that precipitated in an external magnetic field form also some regular structures on the surface of the thin dense LDH film (inset in Figure 8). We associate this phenomenon with orientation effect of a magnetic field on the LDH crystallites—nanoflakes during the precipitation process. Our preliminary calculations revealed a highly anisotropic magnetic susceptibility of Co-containing octahedral layers that leads to a predominant space orientation of the LDH nanoflakes in a magnetic field.

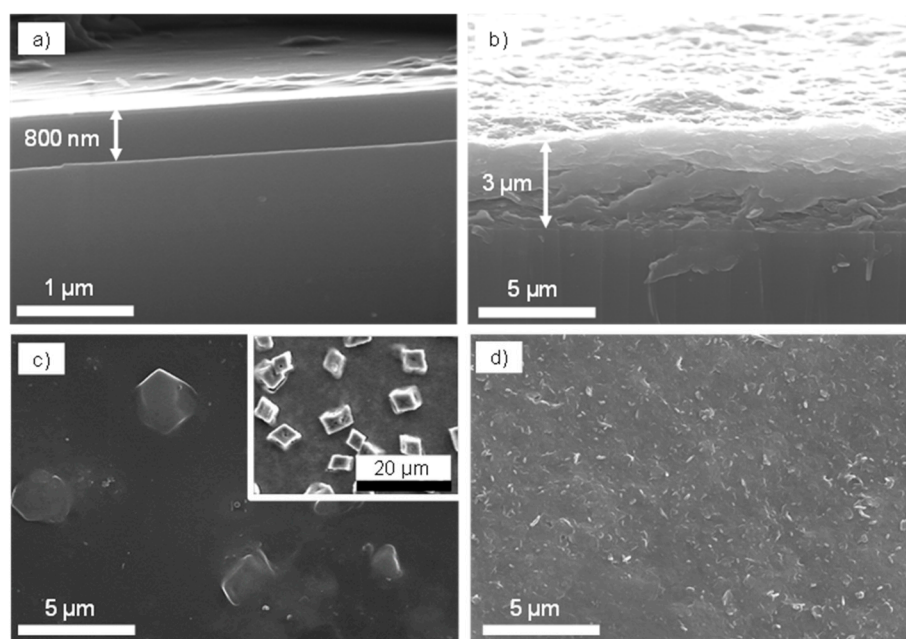


Figure 8. SEM images of layers of the $\text{Co}_2\text{Al-NO}_3$ LDH crystallites deposited on glass substrates with (a,c) and without (b,d) application of an external magnetic field; cross section views (a,b) and top views (c,d). Inset shows the regular-shape particles of $\text{Co}_2\text{Al-NO}_3$ formed on the surface of dense LDH film.

4. Conclusions

The use of high-power sonication for the production of layered double hydroxides emerges as a good option for optimization and improvement of the quality of LDH production.

When high-power sonication was applied to accelerate the processes of the $\text{Co}_2\text{Al-NO}_3$ LDH crystallization and the nitrate-to-carbonate anion-exchange, it was possible to reduce the duration of these processes from 4 h to 5 min (crystallization) and from 7 days to 7 min (anion exchange).

The magnetic field assisted approach to the formation of homogeneous oriented layers of de-agglomerated crystallites—flakes of Co^{2+} -containing LDHs—is promising and deserves further development and optimization. Although crystallites of Co_2Al LDHs are typically small and inclined to agglomeration that makes the studies related to their magnetic anisotropy difficult, they can be dispersed and precipitated as ordered layers in an external magnetic field. Semi-transparent samples of 0.15–0.30 mm thick with relatively big blocks (up to 0.5 mm wide) of ordered LDH crystallites are obtained from thick layers precipitated and then pressed into compacts. Thin transparent dense films of Co_2Al LDHs are formed from ordered crystallites precipitated from diluted suspensions.

Author Contributions: A.N.S. proposed the main idea and wrote the manuscript. D.E.L.V. prepared the samples, performed XRD characterization, TEM and STEM studies. I.M.L. and Y.O.S. conducted the optical experiments. E.L.F. and A.V.F. calculated magnetic susceptibility of Co-containing LDH crystallites. Y.G.P. and R.Y.B. justified theoretically the possibility of magnetic field-assisted arrangement of the crystallites. V.V.R. designed the setup for the high-power ultrasound treatment. A.D.S. constructed and calibrated the setup and controlled the sonication-assisted experiments. M.G.S.F. and J.M.V. provided useful discussion and interpretation of the obtained results and coordinated the work.

Funding: The work has been done in frame of the project TUMOCS. This project has received funding from the European Union's Horizon 2020 research and innovation program under the Marie Skłodowska-Curie grant agreement No. 645660. The financial support of P2020 COMPETE and FCT-Portugal through project POCI-01-0145-FEDER-016686—PTDC/CTM-NAN/2418/2014 (NANOCONCOR) is acknowledged as well. The research done in University of Aveiro was also supported by the project CICECO—Aveiro Institute of Materials, FCT Ref. UID/CTM/50011/2019, financed by national funds through the FCT/MCTES.

Acknowledgments: D.E.L.V. acknowledges the financial support of this work through the AdvaMtech PhD program scholarship (grant PD/BD/143033/2018).

Conflicts of Interest: The authors declare no conflict of interest.

References

1. Mills, S.; Christy, A.; Génin, J.; Kameda, T.; Colombo, F. Nomenclature of the hydrotalcite supergroup: Natural layered double hydroxides. *Miner. Mag.* **2012**, *76*, 1289–1336. [[CrossRef](#)]
2. Evans, D.G.; Slade, R.C.T. Structural aspects of Layered Double Hydroxides. *Struct. Bond.* **2006**, *119*, 1–87.
3. Rives, V. *Double Hydroxides: Present and Future*; Nova Science Publishers Inc.: New York, NY, USA, 2001; 439p.
4. Newman, S.P.; Jones, W. Layered Double Hydroxides as Templates for the Formation of Supramolecular Structures. In *Supramolecular Organization and Materials Design*; Jones, W., Rao, C.N.R., Eds.; Cambridge University Press: Cambridge, UK, 2001; pp. 295–331.
5. Serdechnova, M.; Salak, A.N.; Barbosa, F.S.; Vieira, D.E.L.; Tedim, J.; Zheludkevich, M.L.; Ferreira, M.G.S. Interlayer intercalation and arrangement of 2-mercaptobenzothiazolate and 1,2,3-benzotriazolate anions in layered double hydroxides: In situ x-ray diffraction study. *J. Solid State Chem.* **2016**, *233*, 158–165. [[CrossRef](#)]
6. Miyata, S. The syntheses of hydrotalcite-like compounds and their structures and physico-chemical properties-I: The Systems $Mg^{2+}-Al^{3+}-NO_3^-$, $Mg^{2+}-Al^{3+}-Cl^-$, $Mg^{2+}-Al^{3+}-ClO_4^-$, $Ni^{2+}-Al^{3+}-Cl^-$ and $Zn^{2+}-Al^{3+}-Cl^-$. *Clays Clay Miner.* **1975**, *23*, 369–375. [[CrossRef](#)]
7. Miyata, S.; Okada, A. Synthesis of hydrotalcite-like compounds and their physico-chemical properties—The system $Mg^{2+}-Al^{3+}-SO_4^{2-}$ and $Mg^{2+}-Al^{3+}-CrO_4^{2-}$. *Clays Clay Miner.* **1977**, *25*, 14–18. [[CrossRef](#)]
8. Miyata, S.; Kimura, T. Synthesis of new hydrotalcite-like compounds and their physicochemical properties. *Chem. Lett.* **1973**, *2*, 843–848. [[CrossRef](#)]
9. Xu, Z.P.; Zeng, H.C. Abrupt structural transformation in hydrotalcite-like compounds $Mg_{1-x}Al_x(OH)_2(NO_3)_x \cdot nH_2O$ as a continuous function of nitrate anions. *J. Phys. Chem. B* **2001**, *105*, 1743–1749. [[CrossRef](#)]
10. Salak, A.N.; Tedim, J.; Kuznetsova, A.I.; Vieira, L.G.; Ribeiro, J.L.; Zheludkevich, M.L.; Ferreira, M.G.S. Thermal behavior of layered double hydroxide Zn-Al-pyrovandate: Composition, structure transformations, and recovering ability. *J. Phys. Chem. C* **2013**, *117*, 4152–4157. [[CrossRef](#)]
11. Mishra, G.; Dash, B.; Pandey, S. Layered double hydroxides: A brief review from fundamentals to application as evolving biomaterials. *Appl. Clay Sci.* **2018**, *153*, 172–186. [[CrossRef](#)]
12. Cunha, V.R.R.; De Souza, R.B.; Da Fonseca Martins, A.M.C.R.P.; Koh, I.H.J.; Constantino, V.R.L. Accessing the biocompatibility of layered double hydroxide by intramuscular implantation: Histological and microcirculation evaluation. *Sci. Rep.* **2016**, *6*, 30547. [[CrossRef](#)]
13. Evans, D.G.; Duan, X. Preparation of layered double hydroxides and their applications as additives in polymers, as precursors to magnetic materials and in biology and medicine. *Chem. Comm.* **2006**, *5*, 485–496. [[CrossRef](#)] [[PubMed](#)]
14. Nalawade, P.; Aware, B.; Kadam, V.J.; Hirlekar, R.S. Layered double hydroxides: A review. *J. Sci. Ind. Res.* **2009**, *68*, 267–272.
15. Neves, C.S.; Bastos, A.C.; Salak, A.N.; Sarykevich, M.; Rocha, D.; Zheludkevich, M.L.; Cunha, A.; Almeida, A.; Tedim, J.; Ferreira, M.G.S. Layered double hydroxide clusters as precursors of novel multifunctional layers: A bottom-up approach. *Coatings* **2019**, *9*, 328. [[CrossRef](#)]

16. Carneiro, J.; Caetano, A.F.; Kuznetsova, A.; Maia, F.; Salak, A.N.; Tedim, J.; Scharnagl, N.; Zheludkevich, M.L.; Ferreira, M.G.S. Polyelectrolyte-modified layered double hydroxide nanocontainers as vehicles for combined inhibitors. *RSC Adv.* **2015**, *5*, 39916–39929. [[CrossRef](#)]
17. Poznyak, S.K.; Tedim, J.; Rodrigues, L.M.; Salak, A.N.; Zheludkevich, M.L.; Dick, L.F.P.; Ferreira, M.G.S. Novel inorganic host layered double hydroxides intercalated with guest organic inhibitors for anticorrosion applications. *ACS Appl. Mater. Interfaces* **2009**, *1*, 2353–2362. [[CrossRef](#)]
18. Wang, Y.; Yan, D.; Hankari, S.; El Zou, Y.; Wang, S. Recent progress on layered double hydroxides and their derivatives for electrocatalytic water splitting. *Adv. Sci.* **2018**, *5*, 1800064. [[CrossRef](#)] [[PubMed](#)]
19. Zou, X.; Goswami, A.; Asefa, T. Efficient noble metal-free (electro) catalysis of water and alcohol oxidations by zinc–cobalt layered double hydroxide. *J. Am. Chem. Soc.* **2013**, *135*, 17242–17245. [[CrossRef](#)]
20. Goh, K.H.; Lim, T.T.; Dong, Z. Application of layered double hydroxides for removal of oxyanions: A review. *Water Res.* **2008**, *42*, 1343–1368. [[CrossRef](#)]
21. Salak, A.N.; Lisenkov, A.D.; Zheludkevich, M.L.; Ferreira, M.G.S. Carbonate-free Zn-Al (1:1) layered double hydroxide film directly grown on zinc-aluminum alloy coating. *ECS Electrochem. Lett.* **2014**, *3*, C9–C11. [[CrossRef](#)]
22. Vicente, P.; Pérez-Bernal, M.E.; Ruano-Casero, R.J.; Ananias, D.; Almeida Paz, F.A.; Rocha, J.; Rives, V. Luminescence properties of lanthanide-containing layered double hydroxides. *Micropor. Mesopor. Mater.* **2016**, *226*, 209–220. [[CrossRef](#)]
23. Smalenskaite, A.; Vieira, D.E.L.; Salak, A.N.; Ferreira, M.G.S.; Katelnikovas, A.; Kareiva, A. A comparative study of co-precipitation and sol-gel synthetic approaches to fabricate cerium-substituted Mg-Al layered double hydroxides with luminescence properties. *Appl. Clay Sci.* **2017**, *143*, 175–183. [[CrossRef](#)]
24. Smalenskaite, A.; Salak, A.N.; Kareiva, A. Induced neodymium luminescence in sol-gel derived layered double hydroxides. *Mendeleev Commun.* **2018**, *28*, 493–494. [[CrossRef](#)]
25. Intissar, M.; Segni, R.; Payen, C.; Besse, J.P.; Leroux, F. Trivalent cation substitution effect into layered double hydroxides $\text{Co}_2\text{Fe}_y\text{Al}_{1-y}(\text{OH})_6\text{Cl } n\text{H}_2\text{O}$: Study of the local order. Ionic conductivity and magnetic properties. *J. Solid State Chem.* **2002**, *167*, 508–516.
26. Coronado, E.; Galan-Mascaros, J.R.; Martí-Gastaldo, C.; Ribera, A.; Palacios, E.; Castro, M.; Burriel, R. Spontaneous magnetization in Ni-Al and Ni-Fe layered double hydroxides. *Inorg. Chem.* **2008**, *47*, 9103–9110. [[CrossRef](#)]
27. Almansa, J.J.; Coronado, E.; Martí-Gastaldo, C.; Ribera, A. Magnetic properties of $\text{Ni}^{\text{II}}\text{Cr}^{\text{III}}$ layered double hydroxide materials. *Eur. J. Inorg. Chem.* **2008**, *2008*, 5642–5648. [[CrossRef](#)]
28. Coronado, E.; Martí-Gastaldo, C.; Navarro-Moratalla, E.; Ribera, A. Intercalation of $[\text{M}(\text{ox})_3]^{3-}$ ($\text{M} = \text{Cr}, \text{Rh}$) complexes into $\text{Ni}^{\text{II}}\text{Fe}^{\text{III}}$ -LDH. *Appl. Clay Sci.* **2010**, *48*, 228–234. [[CrossRef](#)]
29. Giovannelli, F.; Zaghrioui, M.; Autret-Lambert, C.; Delorme, F.; Seron, A.; Chartier, T.; Pignon, B. Magnetic properties of Ni(II)-Mn(III) LDHs. *Mater. Chem. Phys.* **2012**, *137*, 55–60. [[CrossRef](#)]
30. Abellán, G.; Martí-Gastaldo, C.; Ribera, A.; Coronado, E. Hybrid materials based on magnetic layered double hydroxides: A molecular perspective. *Acc. Chem. Res.* **2015**, *48*, 1601–1611. [[CrossRef](#)]
31. Abellán, G.; Jordá, J.L.; Atienzar, P.; Varela, M.; Jaafar, M.; Gómez-Herrero, J.; Zamora, F.; Ribera, A.; García, H.; Coronado, E. Stimuli-responsive hybrid materials: Breathing in magnetic layered double hydroxides induced by a thermoresponsive molecule. *Chem. Sci.* **2015**, *6*, 1949–1958.
32. Carrasco, J.A.; Cardona-Serra, S.; Clemente-Juan, J.M.; Gaita-Ariño, A.; Abellán, G.; Coronado, E. Deciphering the role of dipolar interactions in magnetic layered double hydroxides. *Inorg. Chem.* **2018**, *57*, 2013–2022. [[CrossRef](#)]
33. Carrasco, J.A.; Abellán, G.; Coronado, E. Influence of morphology in the magnetic properties of layered double hydroxides. *J. Mater. Chem. C* **2018**, *6*, 1187–1198. [[CrossRef](#)]
34. Vieira, D.E.L.; Salak, A.N.; Fedorchenko, A.V.; Pashkevich, Y.G.; Fertman, E.L.; Desnenko, V.A.; Babkin, R.Y.; Čižmár, E.; Feher, A.; Lopes, A.B.; et al. Magnetic phenomena in Co-containing layered double hydroxides. *Low Temp. Phys.* **2017**, *4*, 1214–1218. [[CrossRef](#)]
35. Babkin, R.Y.; Pashkevich, Y.G.; Fedorchenko, A.V.; Fertman, E.L.; Desnenko, V.A.; Prokhvatilov, A.I.; Galtsov, N.N.; Vieira, D.E.L.; Salak, A.N. Impact of temperature dependent octahedra distortions on magnetic properties of Co-containing double layered hydroxides. *J. Magn. Magn. Mater.* **2019**, *473*, 501–504. [[CrossRef](#)]

36. Shao, M.; Wei, M.; Evans, D.G.; Duan, X. Magnetic-field-assisted assembly of CoFe layered double hydroxide ultrathin films with enhanced electrochemical behavior and magnetic anisotropy. *Chem. Commun.* **2011**, *47*, 3171–3173. [[CrossRef](#)] [[PubMed](#)]
37. Shao, M.; Xu, X.; Han, J.; Zhao, J.; Shi, W.; Kong, X.; Wei, M.; Evans, D.G.; Duan, X. Magnetic-field-assisted assembly of layered double hydroxide/metal porphyrin ultrathin films and their application for glucose sensors. *Langmuir* **2011**, *27*, 8233–8240. [[CrossRef](#)] [[PubMed](#)]
38. Bastami, T.R.; Entezari, M.H. Synthesis of manganese oxide nanocrystal by ultrasonic bath: Effect of external magnetic field. *Ultrason. Sonochem.* **2012**, *19*, 830–840. [[CrossRef](#)]
39. Caruso, R.A.; Ashokkumar, M.; Grieser, F. Sonochemical formation of colloidal platinum. *Colloids Surf. A Physicochem. Eng. Asp.* **2000**, *16*, 219–225. [[CrossRef](#)]
40. Pradhan, A.; Jones, R.C.; Caruntu, D.; O'Connor, C.J.; Tarr, M.A. Gold-magnetite nanocomposite materials formed via sonochemical methods. *Ultrason. Sonochem.* **2008**, *15*, 891–897. [[CrossRef](#)]
41. Kesavan, V.; Sivanand, P.S.; Chandrasekaran, S.; Koltypin, Y.; Gedanken, A. Catalytic aerobic oxidation of cycloalkanes with nanostructured amorphous metals and alloys. *Angew. Chem. Int. Ed.* **1999**, *38*, 3521–3523. [[CrossRef](#)]
42. Bang, J.H.; Suslick, K.S. Applications of ultrasound to the synthesis of nanostructured materials. *Adv. Mater.* **2010**, *22*, 1039–1059. [[CrossRef](#)]
43. Radha, A.V.; Vishnu Kamath, P.; Shivakumara, C. Order and disorder among the layered double hydroxides: Combined Rietveld and DIFFaX approach. *Acta Cryst. B* **2007**, *63*, 243–250. [[CrossRef](#)] [[PubMed](#)]
44. Johnsen, R.E.; Krumeich, F.; Norby, P. Structural and microstructural changes during anion exchange of CoAl layered double hydroxides: An in situ X-ray powder diffraction study. *J. Appl. Cryst.* **2010**, *43*, 434–447. [[CrossRef](#)]



© 2019 by the authors. Licensee MDPI, Basel, Switzerland. This article is an open access article distributed under the terms and conditions of the Creative Commons Attribution (CC BY) license (<http://creativecommons.org/licenses/by/4.0/>).